

Electrical Impedance Potential Mammography for Visualization of Objects (Electrochemical Tests)

A Karpov^{1,2}, M Korotkova^{1,2}, Yu Tsوفин² and V Tsyplyonkov² and M Machin²

¹Clinical Hospital 9, Yaroslavl, Russia

²“SIM Technika” PKF, Yaroslavl, Russia

E-mail: kb9@mail.ru
sim-tech@net76.ru

Abstract. The article presents the result of the electrochemical testing of the potential electric impedance mammograph “MEIK” (version 5.6) which reconstructs the image using the reciprocal projection method. The testing was carried out on several categories: biological objects visualization, definition size, location, depth and shape of the biological objects, concentration and electrical conductivity, resolution capability. The research has been conducted in the original tank filled with homogeneous and heterogeneous medium. The research of the visualization of abiological and bialogical objects, objects dimensions, objects location, objects structure. According to the data of the electrochemical testing, the resolution capability of the objects with high electrical conductivity ranges from 1 to 3 mm and of the objects with low electrical conductivity – from 3 to 5 mm. Due to the given electrochemical testing results potential electric impedance mammograph “MEIK” (version 5.6) can be rated as the medical visualization device.

1. Introduction

Nowadays the method of electric impedance potential mammography quite rapidly penetrates into medical practice. Thanks to the completion of clinical trials high informativity of this method was shown both for oncological diagnostic and for diagnostic of nonneoplastic diseases of the memmary gland. Quite wonderfully clinical trials were conducted prior to laboratory tests. The article demonstrates some results of the electrochemical tests of electrical impedance potential mammograph MEIK v. 5.6, in which backprojection method is used to reconstruct the image.

2. Methodology

Impedance tomograms were obtained by means of electrical impedance potential mammograph MEIK v. 5.6 (50 kHz, 0.5 mA) with single-plane placement of electrodes. An original tank with a base electrode was used for the placement of solutions and objects of interest. Computer scanning was performed each 8 mm to the maximum depth 46 mm (seven scan planes). The results were processed by means of descriptive statistics methods.

3. Backprojection algorithm

The backprojection algorithm is based on the simple fact described below. Changing the conductivity of elemental volume of a medium results in a change of surface potential difference located in a bounded area. This area is a projection of the original elementary volume to the measurement surface

along the equipotential surfaces. Our modification of the backprojection algorithm is based on the work [2]. Under this approach, the conductivity $\sigma(r)$ in point r is estimated as:

$$\sigma(r) = 1 + w_z(s) \cdot S(r),$$

$$S(r) = \sum_j P(r, j) \cdot \frac{R(\bar{r}, j, Q)}{R(\bar{r}, j, Q^*)} \quad R(\bar{r}, j, Q) = \int_{c(r, j)} w(|\bar{r} - \bar{q}|) \cdot Q[D(j, \bar{q})] d\bar{q}, \quad D(j, \bar{q}) = \frac{E_o^j(\bar{q}) - E^j(\bar{q})}{E_o^j(\bar{q})},$$

where $w_z(s)$ - weight function that takes into account the decrease of sensitivity with depth; j - number of inducing electrode; $P(r, j)$ - regularization operator, which takes into account the change in sensitivity depending on the distance from the inducing electrode; $Q(s)$, $Q'(s)$ - regularization operators, taking into account the different reliability of the different values of relative change of electric field; $c(r, j)$ - intersection of the measurement surface with equipotential surface built for the j -th induction electrode and passing through the point r ; $w(s)$ - weighting function that takes into account the decrease of sensitivity with distance from the point r ; E^j - electric field to the measured surface potential; E_o^j - reference electric field for surface potential, measured for homogeneous medium. Electric field is calculated as surface potential gradient projection to the line of integration.

4.Result

The article demonstrates the results of the tests which were conducted in a homogeneous medium, which is moderately hard water (less than 10 mmol/l) or amylose aqueous solution (50 g/l). The objects were placed at 1-3 cm depth. Electrochemical tests were conducted for such categories: visualization of abiological and biological objects, objects dimensions, objects location, objects structure.

4.1 Visualization of Abiological Objects of Different Electrical Conductivity

The objects of different electrical conductivity (a coin and a rubber ball) are represented in figure 1. The object which has high electrical conductivity (the coin, 25 mm in diameter) can be visualized as a hypoechoic mass. The object which possesses low electrical conductivity (the rubber ball, 2 cm in

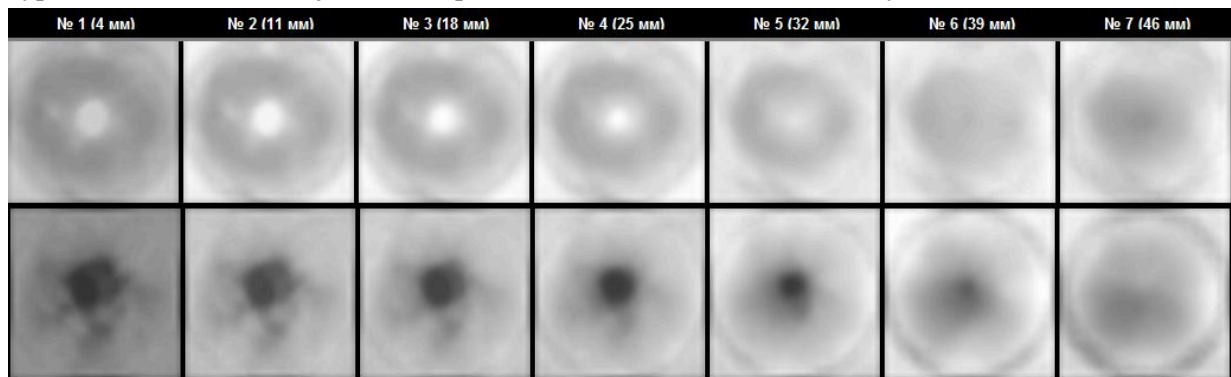
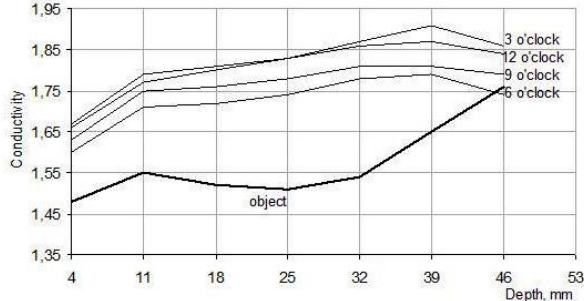


Figure 1. Visualization of abiological objects of different electrical conductivity. In the upper row there is the image of the coin (the object of high electrical conductivity). In the upper row there is the image of the rubber ball (the object of low electrical conductivity).

diameter) can be visualized as a hyperechoic mass. Certain blurring of the objects' contours, which impedes its sizing and locating. Additional image processing (inversion, color gamma) allows acquiring a more sharp contour of the object. The size of the object and the depth of its location can be measured by means of electrical conductivity trend on the scan planes. On the graph (graph 1), which demonstrates the trend of electrical conductivity on the scan planes with the image of the rubber ball (figure 1) at the depth 11-32 mm the area of the decreased electrical conductivity can be clearly

visualized. It is evoked by the object approximately sized 21 mm. Electrical conductivity around the object (at 3, 6, 9 and 12 on the clock dial) tends to increase constantly.



Graph. 1. Trend of electrical conductivity on the scan planes with the image of the rubber ball. The negative extremum corresponds to the location of the object.

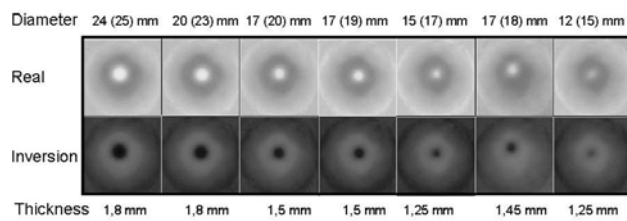


Figure 2. Electrical impedance images of coins of different size and thickness, made from alloy of steel, nickel and copper (the real dimensions of the coins are indicated in brackets in the first row).

inversely proportional to its cross-sectional area. The thickness of the coin influences the location of extremum on electrical conductivity trend (graph 2). These features should be used to more precise definition of the objects' depth; a fortiori the so-called "long-tailed trains" of the image can be visualized on the scan planes. These "long-tailed trains" occupy 2-3 scan planes and influence the accuracy of measurements.

4.3 Visualization of Biological Objects of Different Electrical Conductivity

The figure 3 represents the biological objects of different electrical conductivity. The upper row

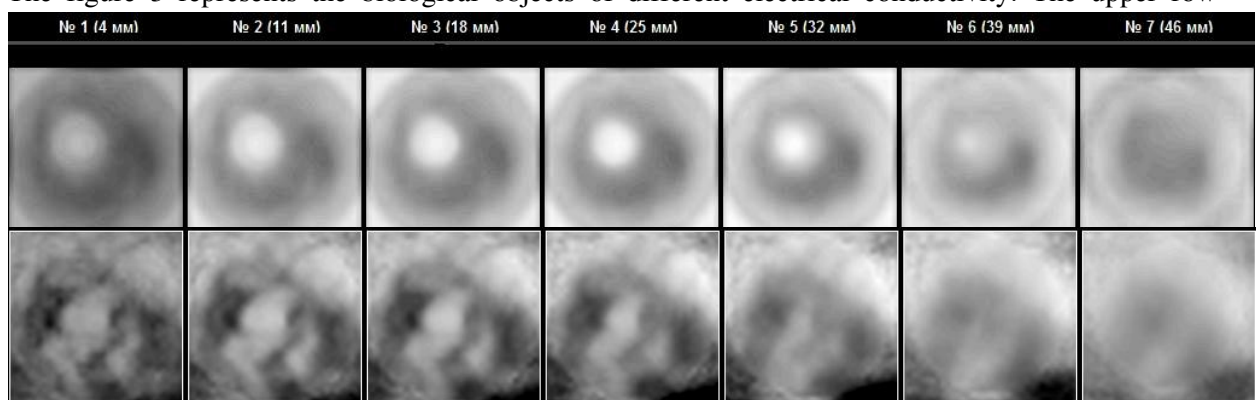
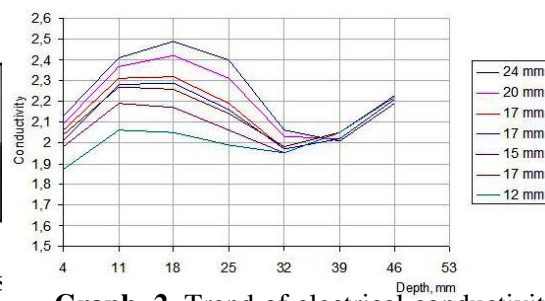


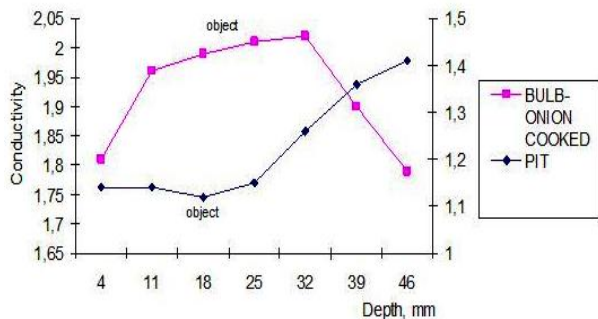
Figure 3. Visualization of biological objects of different electrical conductivity: The upper row represents the image of an onion cooked sized 27x31 mm, the lower row depicts an apple pit sized 7x3 mm.

4.2 Visualization of Abiological Objects of Different Size

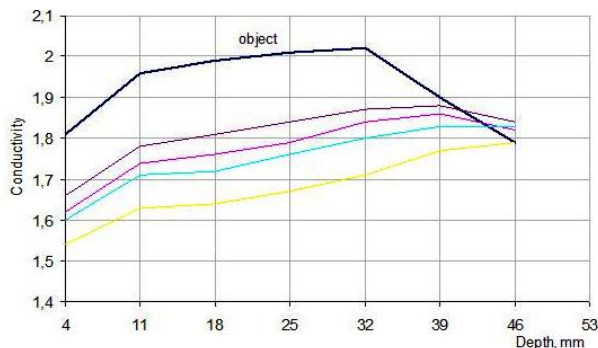
The figure 2 represents the images of coins of different size and thickness, made from alloy of steel, nickel and copper. The depth of the image plane is 11 mm. More sharp contours of the objects are acquired by means of inversion. The size of the images is somewhat smaller than the real size of the coins (the real sizes of the coins are indicated in brackets in the figure 2). We found out that the increase of coins' sizes results in electrical conductivity increase – the fact which correspond to the theoretical data: resistance of an object is



Graph. 2. Trend of electrical conductivity on the scan planes with the images of coins. The positive extremum corresponds to the location of the object.



Graph. 3. Trend of electrical conductivity on the scan planes with the cooked onion (upper row) and the apple pit (lower row).



Graph. 4. Trend of electrical conductivity of the object and of the surrounding area on the scan planes with the image of the cooked onion.

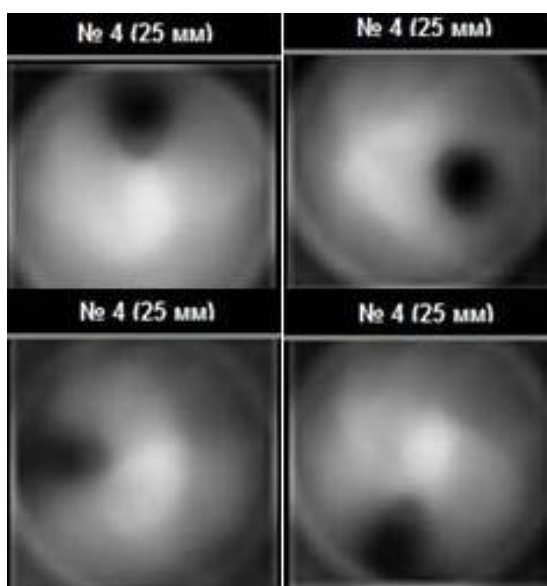


Figure 4. Electrical impedance image of the cooked onion which is moved clockwise (12, 3, 6 and 9 on the clock dial).

represents the image of an onion cooked sized 27x31 mm. The object can be visualized in the center of the image on 5 scan planes as a light round-shaped area (31x34 mm) with high electrical conductivity (hypoimpedance effect). The lower row depicts an apple pit sized 7x3 mm. The object can be visualized in the image on 3 scan planes at 9 on the clock dial as a dark round-shaped area (10x7 mm) with low electrical conductivity (hyperimpedance effect). The depth of object's location can measured using electrical conductivity trend on the scan planes (graph 3). Positive extremum at 11-32 mm depth and negative extremum at 18 mm depth corresponds to the location of the biological objects: the cooked onion and the apple pit respectively. That said electrical conductivity around the object (graph 4), in the example cited it is a cooked onion, tends to increase constantly.

4.4 Objects Location

Changing of the location of the objects causes the changes of electrical conductivity. The figure 4 represents the image of the biological object (an onion cooked) which is moved clockwise. The object sized 34x31 mm was placed at 20 mm depth. The electrical impedance images are represented by the 4th inverse scan plane (25 mm). The object can be visualized as a dark round-shaped area (31x27 mm). Changing of the object location causes corresponding changes of the location of the high electrical conductivity area.

4.5 Visualization of Biological Objects of Different Size

Biological objects of different size, as well as abiological objects, can be visualized by means of electrical impedance potential mammography. But there is a significant difference: real dimensions of biological objects are smaller than the size of their electrical impedance images, while in the case of abiological objects the situation is quite the contrary. There are actual and inverse electrical impedance images of two onions (raw and cooked) in the figure 5. A light round-shaped area sized 27x30 mm can be visualized on the image at 3 on the clock dial which corresponds with the location of the cooked onion sized 20x25 mm. A light round-shaped area sized 24x17 mm can be visualized on the image at 9 on the clock dial which

corresponds with the location of the raw onion sized 20x13 mm.

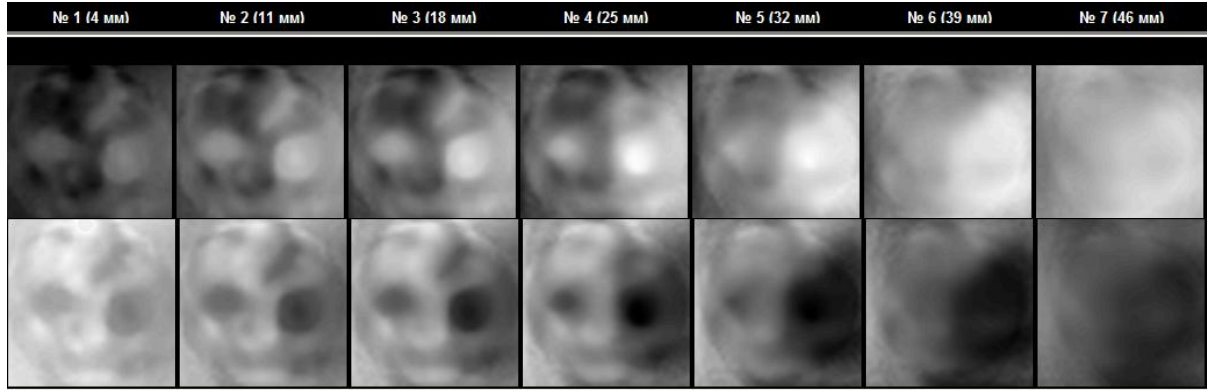


Figure 5. Actual (upper row) and inverse (lower row) electrical impedance images of two onions (raw and cooked) of different size.

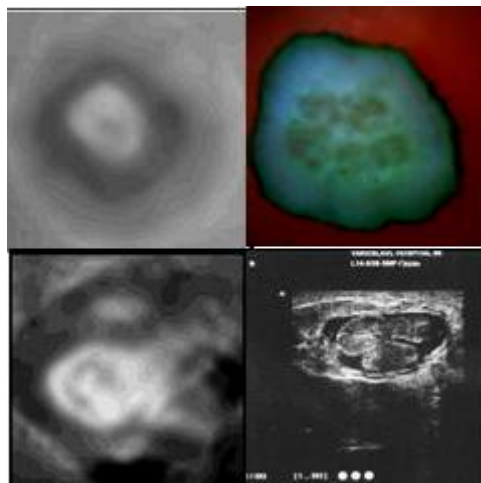


Figure 6. Electrical impedance image of the internal structure of a biological object: the ucumber in the upper row and the breast cancer in the lower row.

(visualization). Whether it is good or bad is a topic in its own right. But the possibility to estimate electrical properties, dimensions and location of biological objects, as well as the capability to identify their internal structure is evidence of its usability. In the meantime the electrochemical tests should be continued both in homogeneous and in heterogeneous mediums. Further development of mathematical algorithms, instruments and software will allow improving image quality, minimizing “long-tailed trains” influence, ensuring adequate accuracy etc.

4.6 Biological Object Structure

If a biological object is close to the array of electrodes (10-20 mm), then it's possible to acquire the electrical impedance image of its internal structure. The figure 6 in the upper row represents the electrical impedance image of a cucumber segment (11 mm depth) and its real image. The hyperimpedance cortical layer can be easily defined. In the center of the image there is the hypoimpedance pulp layer with hyperimpedance septa. The figure in the lower row represents the electrical impedance image (11 mm depth) and the ultrasound image of the mammary tumour. The hypoimpedance liquid component on the periphery of the mass and the heterogeneous hyperimpedance internal structure can be easily observed.

5. Conclusion

We prepared a brief report of electrochemical tests, which were performed by means of electrical impedance potential mammograph MEIK v. 5.6. The obtained during the tests results allow us to consider electrical impedance potential mammography as a means of medical imaging